

## Accepted Manuscript

Title: Rinse-Resistant Superhydrophobic Block Copolymer  
Fabrics by Electrospinning, Electrospaying and  
Thermally-Induced Self-Assembly

Authors: Jie Wu, Xin Li, Yang Wu, Guoxing Liao, Priscilla  
Johnston, Paul D. Topham, Linge Wang

PII: S0169-4332(17)31731-2  
DOI: <http://dx.doi.org/doi:10.1016/j.apsusc.2017.06.076>  
Reference: APSUSC 36276

To appear in: *APSUSC*

Received date: 23-3-2017  
Revised date: 18-5-2017  
Accepted date: 6-6-2017

Please cite this article as: Jie Wu, Xin Li, Yang Wu, Guoxing Liao, Priscilla Johnston, Paul D. Topham, Linge Wang, Rinse-Resistant Superhydrophobic Block Copolymer Fabrics by Electrospinning, Electrospaying and Thermally-Induced Self-Assembly, Applied Surface Science <http://dx.doi.org/10.1016/j.apsusc.2017.06.076>

This is a PDF file of an unedited manuscript that has been accepted for publication. As a service to our customers we are providing this early version of the manuscript. The manuscript will undergo copyediting, typesetting, and review of the resulting proof before it is published in its final form. Please note that during the production process errors may be discovered which could affect the content, and all legal disclaimers that apply to the journal pertain.

# Rinse-Resistant Superhydrophobic Block Copolymer Fabrics by Electrospinning, Electrospraying and Thermally-Induced Self- Assembly

Jie Wu<sup>a</sup>, Xin Li<sup>a,b</sup>, Yang Wu<sup>a</sup>, Guoxing Liao<sup>a</sup>, Priscilla Johnston<sup>c</sup>, Paul D. Topham<sup>c\*</sup>, Linge Wang<sup>a,b\*</sup>

<sup>a</sup> *State Key Laboratory of Luminescent Materials and Devices, School of Materials Science and Engineering, South China University of Technology, Guangzhou 510640, China.*

<sup>b</sup> *South China Advanced Institute for Soft Matter Science and Technology, South China University of Technology, Guangzhou 510640, China.*

<sup>c</sup> *Aston Institute of Materials Research, Aston University, Birmingham, B4 7ET, UK.*

## **Corresponding Authors**

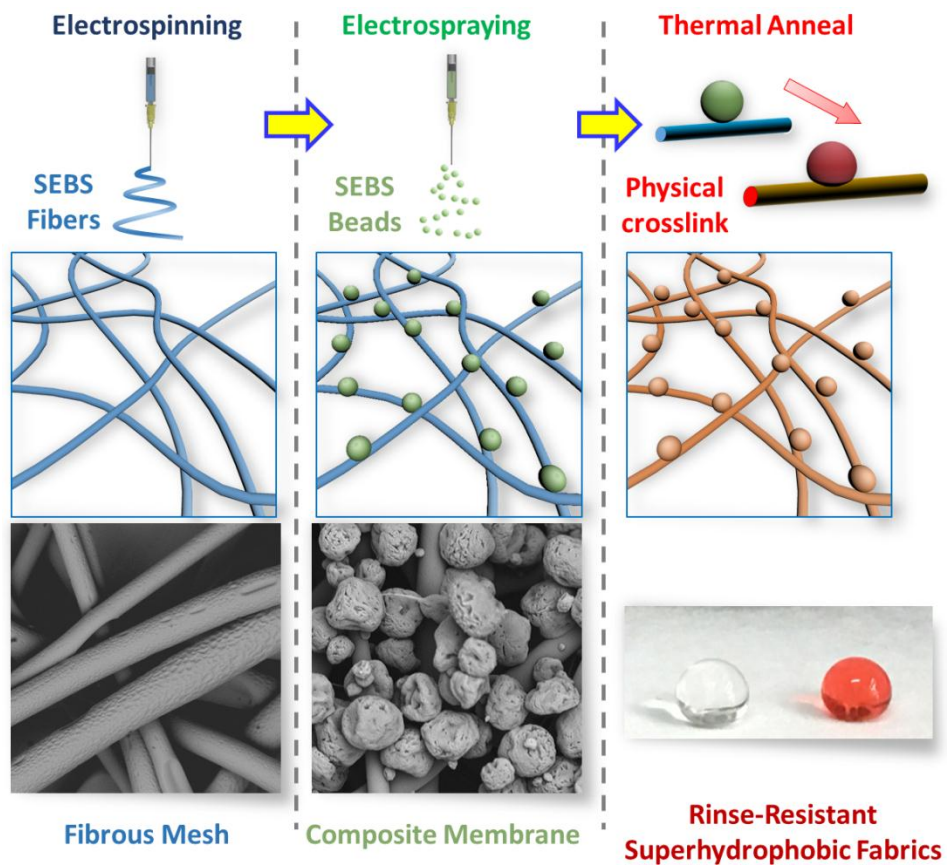
Paul D Topham, Tel.: +44-1212043413. E-mail: [p.d.topham@aston.ac.uk](mailto:p.d.topham@aston.ac.uk)

Linge Wang, Tel.: +86-20-22236077. E-mail: [lingewang@scut.edu.cn](mailto:lingewang@scut.edu.cn);

TOC Graphical abstract

**Rinse-Resistant Superhydrophobic Block Copolymer Fabrics by Electrospinning, Electrospaying and Thermally-Induced Self-Assembly**

We present an efficient approach for the fabrication of superhydrophobic fabrics with great rinse-resistance by electrospinning and electrospaying an elastomeric block copolymer to give a morphologically composite material. Self-assembly of the block copolymer domains was then used to provide long-lasting superhydrophobic property.



## Highlights

- Fabrication of superhydrophobic fibrous fabrics by exploiting block copolymer self-assembly to bind electrospayed beads within a nanofibrous electrospun mesh
- Effects of type and density of beads on the surface morphology and wetting properties were elucidated
- Superhydrophobic fibrous fabrics with great rinse-resistance retained after 200 hours of water flushing

**Abstract:** An inherent problem that restricts the practical application of superhydrophobic materials is that the superhydrophobic property is not sustainable; it can be diminished, or even lost, when the surface is physically damaged. In this work, we present an efficient approach for the fabrication of superhydrophobic fibrous fabrics with great rinse-resistance where a block copolymer has been electrospun into a nanofibrous mesh while micro-sized beads have been subsequently electrosprayed to give a morphologically composite material. The intricate nano- and microstructure of the composite was then fixed by thermally annealing the block copolymer to induce self-assembly and interdigitation of the microphase separated domains. To demonstrate this approach, a polystyrene-*b*-poly(ethylene-*co*-butylene)-*b*-polystyrene (SEBS) nanofibrous scaffold was produced by electrospinning before SEBS beads were electrosprayed into this mesh to form a hierarchical micro/nanostructure of beads and fibers. The effects of type and density of SEBS beads on the surface morphology and wetting properties of composite membranes were studied extensively. Compared with a neat SEBS fibrous mesh, the composite membrane had enhanced hydrophobic properties. The static water contact angle increased from 139° ( $\pm 3^\circ$ ) to 156° ( $\pm 1^\circ$ ), while the sliding angle decreased to 8° ( $\pm 1^\circ$ ) from nearly 90°. In order to increase the rinse-resistance of the composite membrane, a thermal annealing step was applied to physically bind the fibers and beads. Importantly, after 200 hours of water flushing, the hierarchical surface structure and superhydrophobicity of the composite membrane were well retained. This work provides a new route for the creation of superhydrophobic fabrics with potential in self-cleaning applications.

**Keywords:** superhydrophobic; composite membrane; rinse-resistance; block copolymer; self-assembly

## 1. Introduction

Superhydrophobic materials have surfaces with water contact angles (CAs) larger than  $150^\circ$  and sliding angles of less than  $10^\circ$ . They have been used in many applications including self-cleaning,[1-5] oil-water separation,[6-9] antifreeze,[10, 11] and antibacterial materials[12-14]. Two of the most important factors governing the wettability of materials are surface energy and surface roughness, with hierarchical micro/nanostructures and low surface-energy materials being essential in achieving superhydrophobicity.[1, 15] Various methods have been explored to fabricate superhydrophobic surfaces, such as inorganic nanoparticle surface coatings,[16] electrochemical polymerization,[17] plasma-etching,[18] template/mold methods,[19] electrospinning[1, 20-25] and others.[26]

Electrospinning is a relatively simple, efficient and versatile way to fabricate continuous fibers from a variety of materials for wide ranging applications.[23, 27-34] Fibers, beads or beaded structures can be electrospun or electrospayed from polymer solutions with low concentrations or low molecular weight,[35] or *via* specialized self-assembly driven electrospinning.[36] Both electrospinning and electrospaying operate using the principles of electrohydrodynamics, and are widely applied to fabricate superhydrophobic surfaces. For example, Jiang *et al.*[1] prepared a lotus-leaf-like superhydrophobic surface from a composite film consisting of electrospayed polystyrene (PS) microspheres (beads) and electrospun nanofibers. The hierarchical micro/nanostructure of the composite film displayed stable superhydrophobicity, with the water CA of the composite film ( $162^\circ$ ) being much larger than that of the spin-coated film ( $95^\circ$ ). Zheng *et al.*[22] used electrospinning and electrospaying to produce composite membranes with different surface morphologies, including: beads and fibers of different sizes and shapes, bead-

on-string structures with different aspect ratios. It was shown that morphology greatly influenced the wettability of the membranes, ranging from hydrophobic (CA  $\sim 143^\circ$ ) to superhydrophobic (CA  $\sim 160^\circ$ ). Numerous other reports confirm that electrospun/electrosprayed composite membranes incorporating hierarchical micro/nanostructures can display superhydrophobicity.[37-41] However, an inherent problem that restricts the practical application of these materials is that the superhydrophobicity property is not sustainable. It can be diminished, or even lost, when the surface is physically damaged. In particular, electrospayed beads or particles can be removed from the attached or connected surface by certain aggressive treatments, such as ultrasound, scotch tape, water flow or rubbing.[42] Thus, to retain the integrity of the surface and the interconnection between the fibers and the beads, further stabilizing treatments are required. One way to combine the components is to fabricate fibers and beads using the same thermoplastic polymer and thermally anneal them together.

Herein we introduce a method to fabricate rinse-resistant superhydrophobic fabrics with micro/nanostructural features using a combination of electrospinning, electrospraying and thermal annealing. A triblock copolymer, polystyrene-*b*-poly(ethylene-*co*-butylene)-*b*-polystyrene (SEBS) was first electrospun to fabricate fibers as a base supporting mesh. Subsequently, two different types of SEBS beads were electrosprayed onto the fibrous SEBS mesh to form a morphologically composite membrane with a hierarchical micro/nanostructure. The effects of type and density of the SEBS beads on the surface morphology and the hydrophobicity of composite membrane were studied *via* scanning electron microscopy (SEM), water CA and sliding angle, optical microscopy and 3D morphology measurements. In order to increase the rinse-resistance of the composite membrane, a thermal treatment was applied to entangle (or physically crosslink) the fibers and beads. Importantly, after 200 hours of water

flushing, the hierarchical surface structure and superhydrophobicity of the composite membrane were well retained, thus highlighting their promise in self-cleaning applications.

## 2. Experimental

### 2.1. Materials

Polystyrene-*b*-poly(ethylene-*co*-butylene)-*b*-polystyrene (SEBS) triblock copolymer [ $M_n = 7.06 \times 10^4 \text{ g mol}^{-1}$ , polystyrene (PS) volume fraction:  $\phi = 0.30$ , also known as Kraton G1726M], was obtained from Kraton Performance Polymers, Inc. Tetrahydrofuran (THF) and *N,N*-dimethylformamide (DMF) (Laboratory Grade) were purchased from Aladdin and used as received.

### 2.2. Fabrication of SEBS fibers, bead-fiber composite membranes and thermal annealing treatment

2.2.1. Electrospinning: The SEBS triblock copolymer was dissolved in THF at a concentration of 14 wt%.[36] The solution was then stirred continuously for 24 h prior to electrospinning at 25 °C. Electrospinning was performed at 25 in air, using homemade apparatus similar to that used in the literature.[31, 43] SEBS polymer solution was drawn into a 1 mL syringe connected to a 0.62 mm inner diameter flat-ended metallic needle. The solution was fed at 2 mL h<sup>-1</sup> using a syringe pump (LSP01-1A, Longer precision pump Co., Ltd., China) in a horizontal mount and the needle was connected to a high voltage supply (DW-P303-1ACF0, Dongwen high voltage power supply Co., Ltd., China), fixed at 20 kV. An aluminum flat sheet (10 cm × 10 cm) was grounded and used as the collector. The distance between the needle and collector was fixed at 15 cm. Ambient

humidity was controlled at RH30%, RH50% and RH70%. The electrospinning time was kept constant at 10 min.

2.2.2. Electrospaying: The SEBS triblock copolymer was dissolved in THF at a concentration of 8 wt% or THF/DMF mixed solvent (THF/DMF = 80/20) at 14 wt%.[36] The solutions were then stirred continuously for 24 h prior to electrospaying at 25 °C. The setup and the parameters of electrospaying were exactly same as those used for electrospinning, except the pre-prepared electrospun SEBS fibrous mesh on aluminum sheet was grounded and used as the collector. Ambient humidity was controlled at RH30% and RH70%, respectively. In order to achieve different densities of beads on the fibers, the electrospaying process was undertaken for different time periods (10 min, 20 min, 30 min and 40 min, respectively).[44] For analysis, the electrospun fibers and beads were dried under reduced pressure at room temperature for 24 hours to remove any residual solvent.

2.2.3. Thermal annealing: After electrospaying, the composite membranes comprising fibers and beads, were heated at 170 °C for 3 h to thermally anneal the fibers and beads. [45] The samples were heated without removing the aluminum sheet in order to prevent folding of the SEBS fibrous mesh during the annealing process.[46]

### **2.3 Flushing experiment**

The composite membranes (with size 10 cm × 10 cm) before and after thermal annealing were placed under a faucet at a distance of 20 cm from the source and flushed by swift water flow (1.2 m s<sup>-1</sup>) for different time periods (between 0-200 h).

## 2.4. Characterization

Relative number-average molecular mass ( $M_n$ ) and dispersity ( $M_w/M_n$ ,  $D$ ) were measured by Gel Permeation Chromatography (GPC) (flow rate 1 mL min<sup>-1</sup>, 40 °C) using a Varian GPC spectrometer comprising three PL gel 5 µm 300 x 7.5 mm mixed-C columns and a degassed THF eluent system containing triethylamine (2 % v/v) and BHT (0.05 % w/v). The samples were calibrated with narrow polystyrene standards ( $M_p$  range = 162 to 6 × 10<sup>6</sup> g mol<sup>-1</sup>) and analysed using PL Cirrus software (version 2.0) supplied by Agilent Technologies. The traces and data are provided in the Electronic Supporting Information (ESI), Fig. S1. The surface morphologies of the SEBS fibers and beads were characterized by scanning electron microscopy (SEM), using a Phenom Pro G3 (Phenom, Holland) (operating at 10 kV for gold-coated samples). Average diameters of the fibers and beads produced from each solution were obtained using ImageJ software at least five SEM images. Thermogravimetric analysis (TGA) measurements were conducted by a TG209 F1 (NETZSCH) thermo-analyzer instrument. The heating rate was set at 20 °C min<sup>-1</sup>, and the TGA curves were recorded from 50 to 600 °C under 25 mL min<sup>-1</sup> flow of nitrogen. Approximately 10 mg of sample was used for a single TGA analysis. The errors associated with the temperature and mass measurements were ±2.0 °C and ±2.0%, respectively.

The wettability of the SEBS fibrous mesh, beads and composite membranes were determined by static water contact angle (CA) and sliding angle measurements performed in open air using an OCA20 contact angle system (Dataphysics, Germany). The CA was measured after the DI water droplet (5 µL) had rested for 5 s on the SEBS membranes. All measurements and experiments were performed under ambient conditions (room temperature, 25 °C). The average water CA and sliding angle and their standard deviation were calculated from measurements taken at seven different positions on the same sample.

The surface roughness and topography of SEBS fibrous mesh and composite membranes were measured by a white light interferometer, BMT SMS Expert 3D (BMT, Germany). Interferometry is a non-destructive and non-contact measurement with extremely high sensitivity in Z-direction (vertical resolution of 30 nm).[47] Generally, the scanning area was set at area of 3 mm  $\times$  3 mm with a scanning speed of 1 mm s<sup>-1</sup>. The surface roughness was calculated from the measurements using the BMT system software.

The nanomorphologies of the untreated and thermally annealed SEBS composite membranes (with Type II Beads, 30 min electrospraying) were revealed *via* small-angle x-ray scattering (SAXS). SAXS measurements were performed at the Shanghai Synchrotron Radiation Facility (SSRF), Shanghai, China, on station BL16B[48] (wavelength of x-ray radiation,  $\lambda = 1.24 \text{ \AA}$ , at 10keV) over a  $q$ -range of 0.008 - 0.36  $\text{\AA}^{-1}$  at sample-to-detector distance of 2m (modulus of the scattering vector  $q = 4 \pi \sin\theta/\lambda$ , where  $\theta$  is half of the scattered angle) using a two-dimensional (2D) area detector (SX-165 CCD Detector by Rayonix, LLC, USA.). Peak positions of wet rat-tail collagen were used to calibrate the  $q$ -axis. 2D SAXS patterns have been reduced to one-dimensional (1D) profiles by a standard procedure available in the SAS software package.[49] The 2D patterns, and their corresponding 1D profiles, have been subjected to incident beam intensity and background corrections.

### 3. Results and discussion

Wettability is one of the most important properties of solid surfaces for both academia and industry. For example, there have been numerous reports concerning the development of artificial superhydrophobic surfaces for self-cleaning applications that are inspired by the lotus leaf.[50] Among the various methods used to make superhydrophobic surfaces, electrospinning

is a particularly promising technique to fabricate micro- and nanoscale fibers, as well as different structures and assemblies[51] that display great complexity in terms of surface morphology and topology.[52, 53] Moreover, the fibrous materials obtained from electrospinning can provide porosity for the transport of vapor, essential in a number of applications.[52, 54] Meanwhile, electrospaying, which may be considered a variant of the electrostatic spinning process, is also widely used for generating superhydrophobic surfaces.[37, 38, 41] When polymer or inorganic particles are electrospayed onto a solid substrate, superhydrophobicity can be achieved as a consequence of merely increasing the surface roughness.[18, 38, 42, 55] However, electrospayed particles can be removed from the surface by various aggressive treatments, such as: ultrasound, scotch tape, water flow or surface rubbing.[42] Thus, to retain the integrity of the surface and the interconnection between the fibers and the beads, further modification is required. Herein we report a method to fabricate rinse-resistant superhydrophobic fabrics with hierarchical micro/nanostructure using a combination of electrospinning, electrospaying and thermal annealing (a schematic is given in Fig. 1). SEBS beads were electrospayed onto SEBS fibers to form a composite membrane with a hierarchical micro/nanostructure first, and then thermal treatment was applied to increase the rinse-resistance of the composite membrane by physically binding the beads to the fibrous mesh.

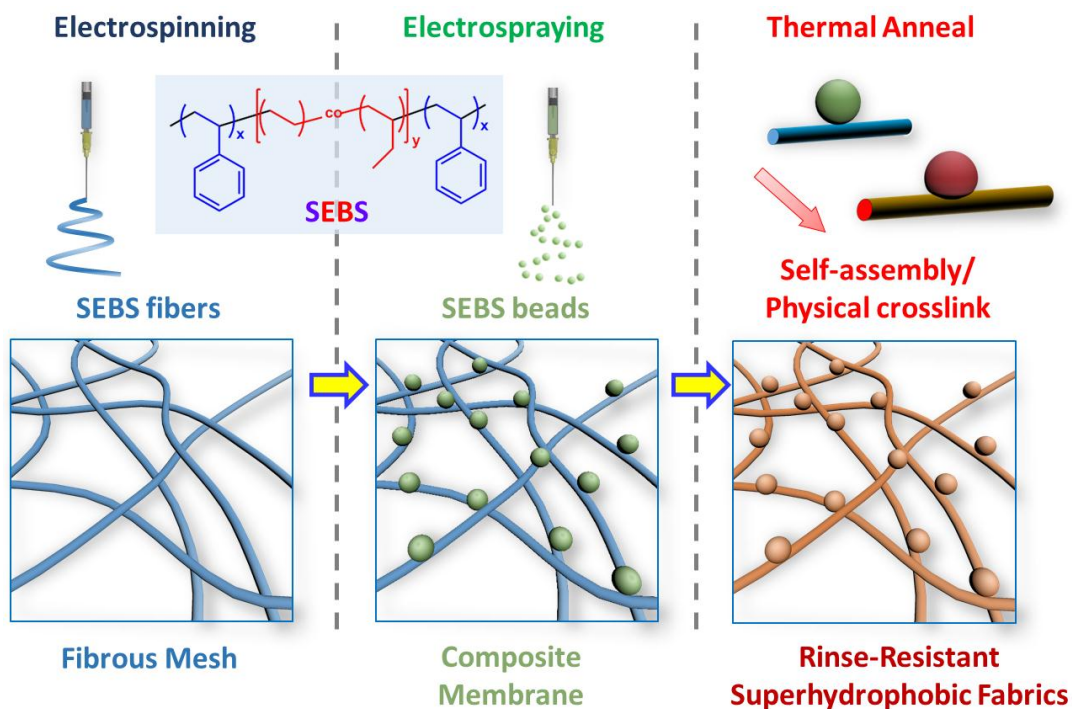


**Fig.1** A schematic illustration of the fabrication process of rinse-resistant superhydrophobic fabrics.

### 3.1. Fabrication of SEBS fibers and beads

In our previous study, SEBS was dissolved in neat THF across a concentration range of 8 - 20 wt% to produce beads or fibers.[36] Based on this work, a solution of 14 wt% SEBS was selected as an optimum concentration to make fibers. It had been reported that high humidity in addition to high solvent volatility often leads to the formation of pores on electrospun fibers.[22] Since surface roughness is key to the fibers' superhydrophobicity, we performed electrospinning at relative humidities of 30, 50 or 70% in order to control the surface morphology of the SEBS fibers. As shown in Fig 2a and 2b, all of the SEBS fibers possessed a cylindrical shape with an average diameter approximately 8 ~ 9  $\mu\text{m}$  (with average diameter approximately  $8.3 \pm 1.1 \mu\text{m}$  at

RH30% and  $9.3 \pm 1.5 \mu\text{m}$  at RH70%, respectively). However, the surface morphology of the fibers changed from smooth to rough (tiny pores appeared on the fiber surface) with increased humidity. In particular, the water CA of the SEBS fibrous meshes increased from  $134^\circ$  to  $142^\circ$  (Fig. 2c). Similar results were reported by Kurusu and Demarquette,[33] with the water CA of the electrospun SEBS fibrous mat was  $139^\circ (\pm 2^\circ)$ . It is believed that the micro/nanostructure of the fibrous meshes (arising from the micrometer-sized fibers and gaps between the fibers, and the nanometer-sized pores on the fiber surface) generates a rough surface, which increases the solid-liquid interfacial area, and therefore increases the apparent surface hydrophobicity. In contrast, SEBS films prepared by casting were smooth (Fig. S2a) and the water CA was much smaller ( $95^\circ$ , as shown in Fig. S2b) than that of the electrospun SEBS fibrous mesh. According to the surface topography measurements, the roughness of the electrospun SEBS fibrous mesh is  $12.1 \mu\text{m}$  while that of the cast film was an order of magnitude smaller at  $1.2 \mu\text{m}$  (Fig. S3).

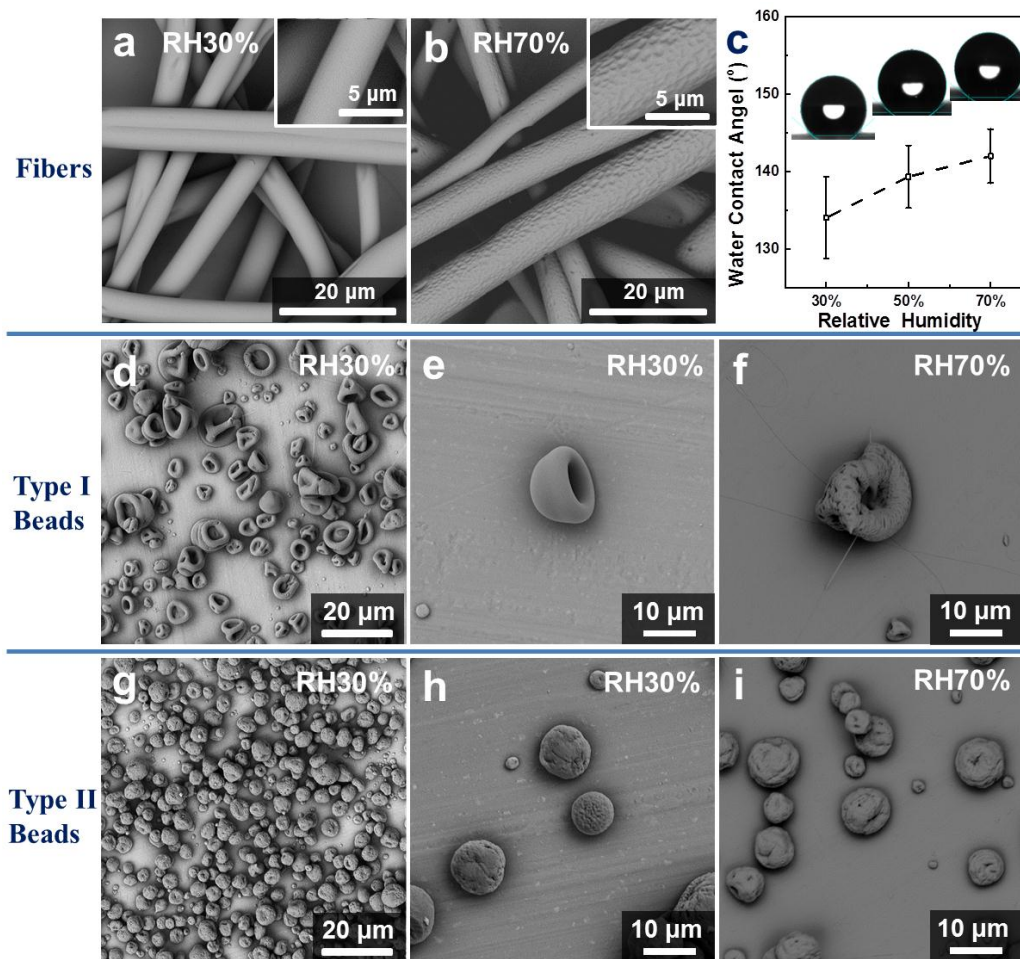


**Fig. 2** SEM images of SEBS fibers electrospun at different humidity; (a) RH30% and (b) RH70%; alongside their water contact angle data (c). Parts (d) to (i) are SEM images of SEBS beads electrospun at different humidity RH30 and RH70%. Type I Beads were fabricated from 8 wt% SEBS/THF solution, while Type II Beads were produced from 14wt% SEBS/THF-DMF (THF/DMF = 80/20) solution. The SEM images shown in (d) and (g) are at low magnifications to provide a larger sample size for the reader.

There are two types of beads that can be prepared from SEBS *via* electrospaying. As shown in Fig. 2d-i, the first type is fabricated from a SEBS solution with low concentration (8 wt%),

named Type I Beads. The second type is produced from the self-assembled block copolymer in a co-solvent system of THF/DMF (80/20) at a high concentration (14 wt%), named Type II Beads.[36] This co-solvent system allows a relatively high polymer concentration to be used, yet with a low degree of entanglement between polymer chains due to microphase separation of the block copolymers (BCP), SEBS, in this selective solvent system.[36] It was noted that Type II Beads were more uniform in size and shape (with an average sphere diameter of approximately  $8.9 \pm 1.8 \mu\text{m}$  at RH30% and  $9.7 \pm 2.3 \mu\text{m}$  at RH70%, respectively) than those produced from THF solutions of low concentration (Type I Beads, size range from 2 ~ 30  $\mu\text{m}$ , with an average diameter of approximately  $21.2 \pm 6.6 \mu\text{m}$  at RH30% and  $22.3 \pm 7.1 \mu\text{m}$  at RH70%, respectively). The effect of humidity on the surface morphology of Type I Beads, was similar to that observed for electrospun SEBS fibers, in that some nanometer-sized pores were generated on the surface of the beads at high humidity (Fig. 2d-f). In contrast, rough surface morphology was always observed for Type II Beads, regardless of humidity (Fig. 2g-i), which was due to the different solvent volatility of THF and DMF and the vapor-induced phase separation effect.[22] Consequently, conditions used to produce Type II Beads were selected for further investigation in the production of hierarchical micro/nanostructure of fiber/bead composite membranes. The effects of the bead density and type on the surface morphology and the superhydrophobic properties of composite membranes are investigated sequentially in the following parts.

### **3.2. Effects of bead density and type on surface morphology and superhydrophobic property of bead/fiber composite membranes**

Bead density has a great effect on the overall surface roughness of composite membranes. The electrospaying process was therefore performed at constant RH30% for different time periods, ranging from 10 min to 40 min, in order to generate membranes consisting of pre-prepared electrospun SEBS fibers (RH70%) and Type II Beads (RH30%). Morphologies of the resulting composite membranes are shown in Fig. 3a-e. The SEM micrographs reveal that beads were stacked on the fibers, and the SEBS composite membranes possessed a hierarchical micro/nanostructure. Fig. 3a shows the bare SEBS fibers without Type II Beads. Images obtained for the membranes prepared by electrospaying for different time periods (10, 20, 30 and 40 min) are shown in Fig. 3b-e, respectively. As expected, the number of beads, counted from the SEM images, confirmed that the density (beads per  $\text{mm}^2$ ) of Type II Beads on the SEBS fibrous mesh increased with electrospaying time (Fig. 3f), from 86,000  $\text{mm}^{-2}$  for 10 min electrospaying to 345,000  $\text{mm}^{-2}$  for 40 min electrospaying.

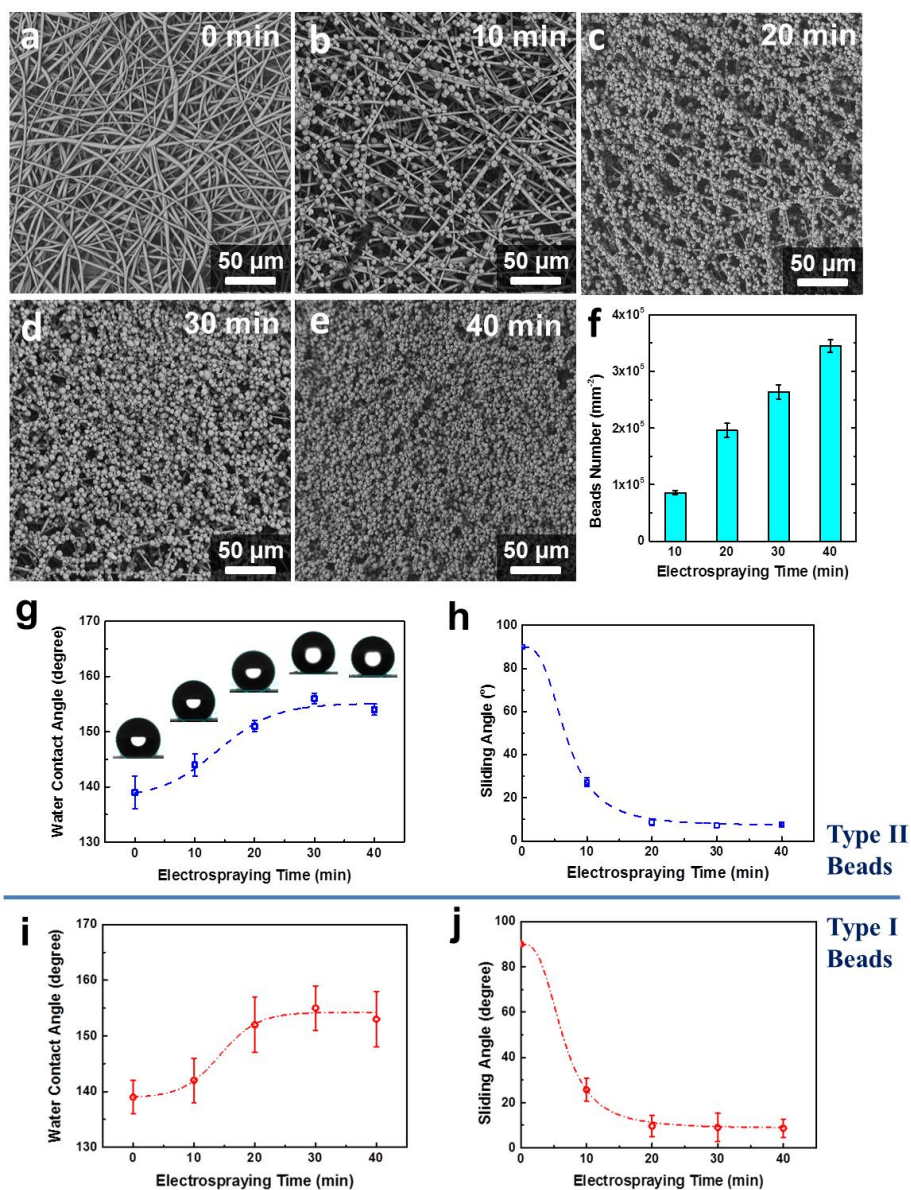


**Fig. 3** SEM images of SEBS composite membrane with different bead density (Type II Beads); (a) 0 min, (b) 10 min, (c) 20 min, (d) 30 min, (e) 40 min and (f) beads density with electrospaying time. Parts (g) and (h) show the corresponding static water contact angle and sliding angle data of the composite membrane of SEBS fibers with Type II Beads, respectively. Parts (i) and (j) show the corresponding static water contact angle and sliding angle data of the composite membrane of SEBS fibers with Type I Beads, respectively.

There are two critical measurements in determining how well the hydrophobic substrate is performing (in self-cleaning); the contact angle and the sliding angle. A higher contact angle means that the surface is more repellent to water, thus requiring less cleaning and maintenance. Lower sliding angles shows that the surface has the ability to allow liquid to be released more quickly, thereby improving cleanability. The water CA and sliding angle data of the composite membranes prepared using Type II Beads are given in Fig. 3 [part (g) and (h)] as a function of electro spray time (*i.e.* bead density). The static water CA of the bare SEBS fibrous mesh was  $139^\circ (\pm 3^\circ)$ , and the sliding angle was nearly  $90^\circ$ . The introduction of SEBS beads caused an increase in the static water CA (Fig. 3g) and a decrease in the sliding angle (Fig. 3h). When Type II Beads were electro sprayed for 30 minutes, the static water CA increased to  $156^\circ (\pm 1^\circ)$ , while the sliding angle decreased to  $8^\circ (\pm 1^\circ)$ , indicating excellent superhydrophobic properties and good for application in self-cleaning. However, continuous packing of the beads did not appear to improve the superhydrophobicity further. Referring to Fig. 3g, the static water CA increased at low-to-moderate bead densities, but reached a plateau at higher bead densities (corresponding to electro spray times of 20/30 min in Fig. 3g). This trend was also reflected in the sliding angle data, except that the sliding angle reduced initially, and reached a minimum at around  $8^\circ$  at higher bead density. These findings imply that the ratio of the wetting phase (beads) to the nonwetting phase of the SEBS composite membranes (air and fibers) was similar for membranes with moderate-to-high bead densities. An electro spray time of 30 mins was found to be optimum in terms of maximum static water CA and minimum sliding angle (Fig. 3h). The SEBS composite membranes with Type I Beads show similar tendency of the effect of the bead density on the superhydrophobic properties of the fibrous membranes (Fig. 3i and 3j). In contrast to

Type II Beads, the static water CA measurements performed on composites with Type I Beads were more broadly distributed (shown in Fig. 3i). It is believed that the nonuniform morphology of the Type I Beads caused greater surface heterogeneity and thus a slightly larger deviation in the water CA measurements (approximately  $155^\circ \pm 4^\circ$  for the sample electrospayed for 30 minutes in Fig. 3i, while that of Type II Beads electrospayed for 30 minutes was  $156^\circ \pm 1^\circ$  in Fig. 3g). The results confirmed that the SEBS composite membranes with Type II Beads have homogeneous surface morphology and more stable performance (superhydrophobicity and wettability).

In order to explain this phenomenon in more detail, a 3D morphology tester was utilized to characterize the roughness of the SEBS fibrous mesh (electrospun fibers only) and composite membranes[47]. The 3D morphology measurement presents a vivid image to reveal the surface morphology with high spatial resolution. Fig. 4a shows the 3D morphology of SEBS fibrous mesh, the violet/blue areas indicate higher sites in the image (showing the arrangement of the fibers on the top of the sample (depicting the stacking of the fibers), while the red/yellow areas show the lower sites or voids. Those measurements revealed a roughness of  $12.1 \mu\text{m}$  for the SEBS fibrous mesh. Fig. 4b-d show 3D morphology images of SEBS composite membranes comprising fibers and Type II Beads. Due to the introduction of beads, the roughness of these composite membranes increased with bead density ( $14.7 \mu\text{m}$ ,  $19.4 \mu\text{m}$  and  $21.8 \mu\text{m}$  for 10, 20 and 30 min electrospaying, respectively). From these data, it appears that the increase in surface roughness arising from incorporation of beads is the main reason for the observed improvements in superhydrophobicity. Meanwhile, the 3D surface topography images show the SEBS composite membranes with Type II Beads had a surface morphology with uniform roughness (over a wide scanning range of  $3 \text{ mm} \times 3 \text{ mm}$ ) than that of the SEBS composite membranes with

Type I Beads ( $21.5\ \mu\text{m}$  for 30 min electrospaying, Fig. S4b), which coincide the result of static water CA data. According to the Cassie-Baxter model, increases in surface roughness and entrapped air lead to a reduction in the ratio of the wetting phase to the nonwetting phase.[37, 56]

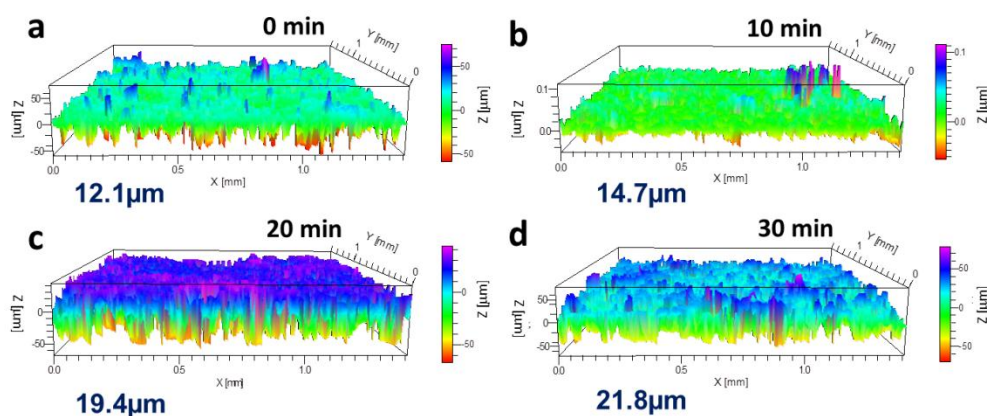


**Fig. 4** 3D surface topography measurements of SEBS composite fibrous membranes with different bead density of Type II Beads (prepared by varying the different electrospaying time).

### 3.3 Flush Properties of SEBS Composite Membrane

It was anticipated that the structure (and therefore superhydrophobicity) of the SEBS composite membranes would not be stable during practical application of the materials because of poor chain entanglement between the fibers and beads. To investigate this, the composite membranes consisting of Type II Beads (electrospayed for 30 min) were tested in flush property trials. Fig. 5c and 5d shows that static water CA of the original composite membrane is about  $156^\circ$ , and the sliding angle is  $8^\circ$ . The membrane was then flushed by swift water flow ( $1.2\ \text{m s}^{-1}$ ), for various time periods (between 0-200 h), and the static CA and sliding angles were measured. After flushing for 200 h, the static CA decreased to  $141^\circ$  and the sliding angle increased to  $77^\circ$ , which

indicated that the membrane lost its superhydrophobicity. SEM revealed that the beads that stacked on the untreated composite membranes (Fig. 5a) were removed after water flushing for 200 h, and only a few beads were retained on the fibrous surface (Fig. 5b). This vast reduction in bead density explains the observed transformation in the membrane's wettability and superhydrophobicity.

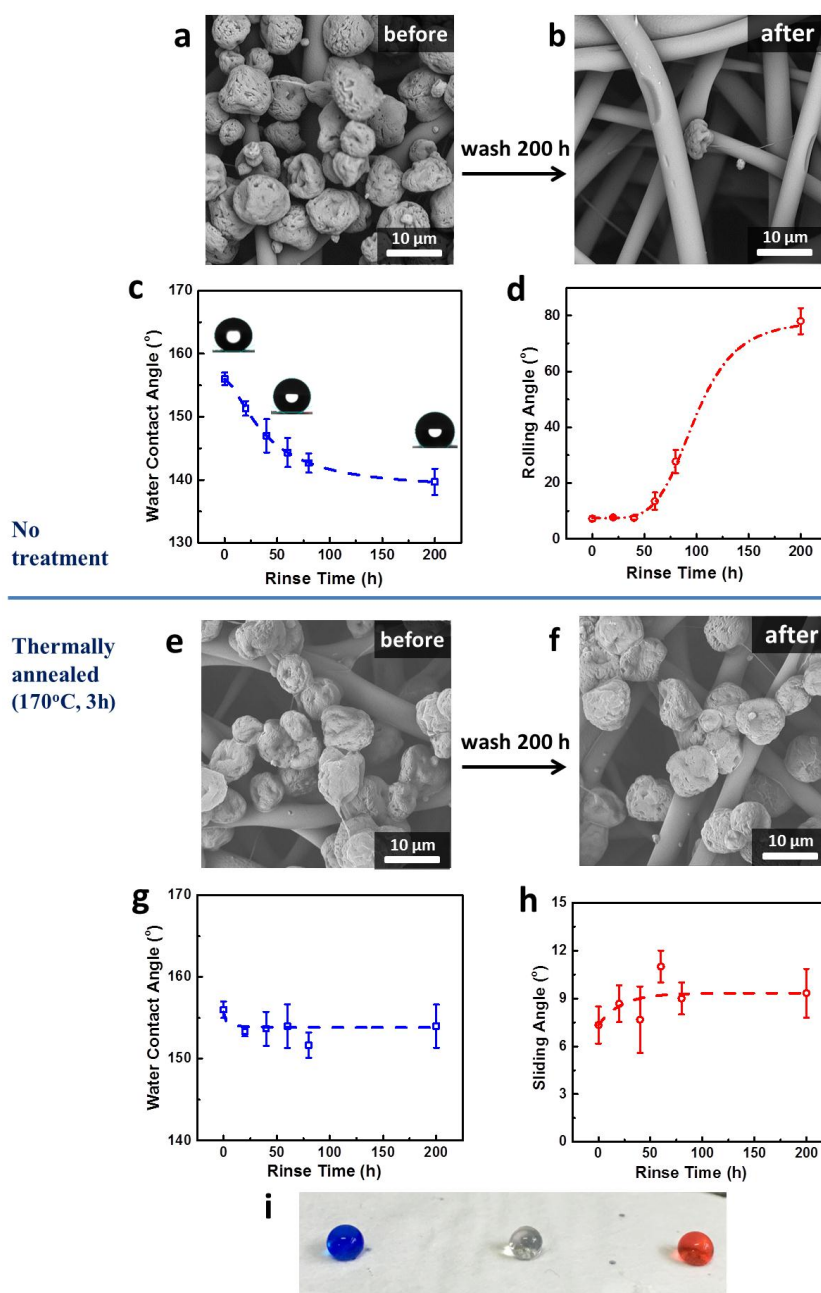


**Fig. 5** SEM images of the untreated (a and b) and thermally annealed (e and f) SEBS composite membranes (with Type II Beads) before and after washing with water (200 h). Parts (c), (d), (g) and (h) are static water contact angle and sliding angle data with different rinse time of the untreated (c and d) and thermal annealed (g and h) SEBS composite membranes (with Type II Beads), respectively. Part (i) shows optical photograph of the thermal annealed SEBS composite membrane with different colored ink droplets.

In order to increase the stability of the composite structure and thus control the surface properties, thermal annealing (170 °C for 3 h) was utilized to increase the mobility and entanglement of molecular chains linking the fibers and beads. Small angle x-ray scattering (SAXS) confirmed that the SEBS chains rearrange (self-assemble) to form a regular nanostructure within the fibers and beads after thermal annealing (see Fig. 6). Moreover, annealing promotes the interdigitation of the SEBS chains, a process which creates physical cross-links between the fibers and beads. This works because the fibers and beads are fabricated from the same polymer; a strategy which has been shown to produce physical crosslinks in various triblock copolymer systems.[57-59] The TGA experiments confirmed that there were no obvious changes in thermal properties following thermal annealing (Fig. S5). After thermal annealing, the composite membrane was subjected to a similar flush experiment. Fig. 5g and 5h show the changes in static water CA and sliding angle of the annealed membrane over the 200 h flushing period. Only minor variations in these angles were detected; after flushing for 200 hours, the static water CA was 154°, and sliding angle was 9°. As revealed by SEM, clearly, the beads and fibers are more intimately linked, which qualitatively supports the concept of physically-crosslinking *via* entanglement of the polymer chains across the fiber-bead interface

(Fig. 5e). Most of the beads remained on the membrane after water flushing (Fig. 5f). Consequently, as shown by our results the structure and superhydrophobicity of the thermally annealed membrane was retained, highlighting their promise as self-cleaning materials.

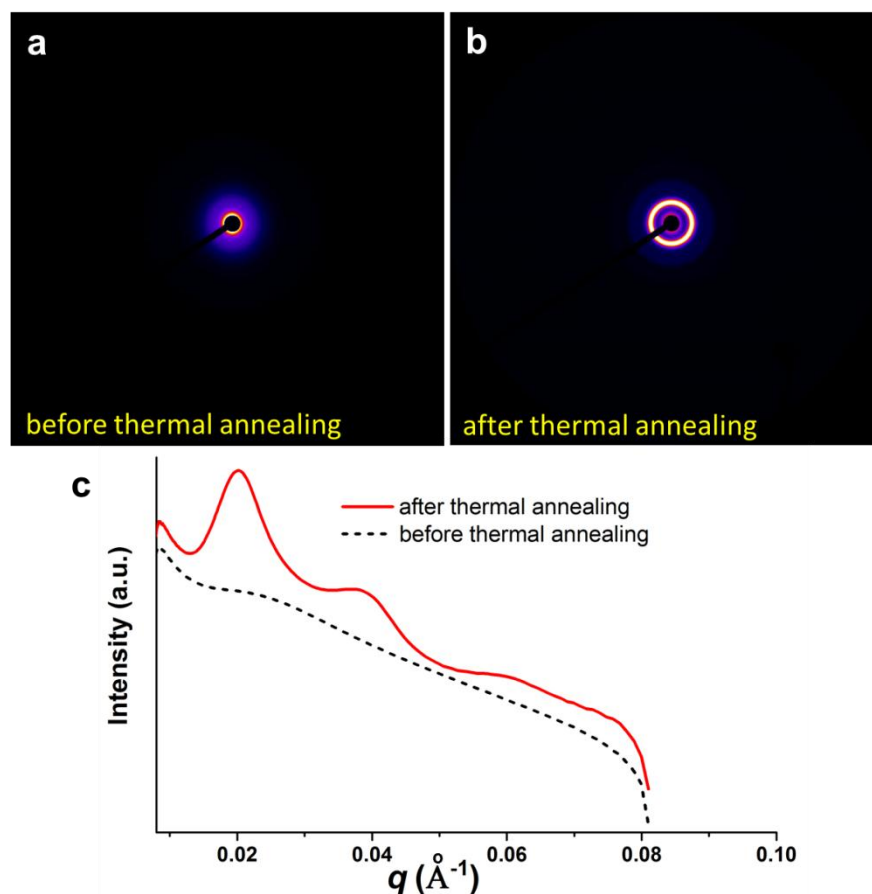


**Figure 6.** Small angle x-ray scattering (SAXS) data of untreated and thermally annealed SEBS composite membranes (with Type II Beads, 30 min electrospinning), where (a) and (b) show the 2D SAXS images and (c) shows the corresponding 1D data of intensity versus  $q$ .

As aforementioned, SAXS was used before and after thermal annealing to further probe the self-assembly/physical crosslinking process of the block copolymer fibers and beads. The almost featureless scattering pattern (Fig. 6a) of the untreated composite membrane indicates that the SEBS chains have been effectively vitrified during the electrospinning (fibers) and

electrospraying (Type II beads) quench processes, as expected. After thermal annealing, the presence of three clear peaks in the SAXS data show that the SEBS chains self-assembled to form a more ordered, regular nanostructure (Fig. 6b). It was found that the relative positions of the first three diffraction peaks ( $q/q^*$  approximately equal to 1, 2, 3, where  $q^*$  is the first peak position in Fig. 6c, which is indicative of a lamellae morphology within the fibers and beads, with an inter-domain spacing of 31 nm).

#### 4. Conclusion

Commercially available Kraton triblock copolymer (SEBS) composite membranes, which consist of fibers and beads, were successfully fabricated by electrospinning and electrospaying. More importantly, block copolymer self-assembly was exploited in the electrospaying process to produce more compact, intact beads with a relatively even size distribution. The introduction of beads successfully increased the static water contact angle of the composite membrane, whilst decreasing the sliding angle dramatically, characteristic of a superhydrophobic material. An increase in density of the SEBS beads on the fibrous mat significantly improved the superhydrophobic properties, while the type of beads dictated the spatial homogeneity of the surface properties. Type II Beads (created through block copolymer self-assembly) were more uniform than Type I Beads in size and shape, which thus led to more homogeneous wettability across the sample surface. After thermal annealing, the composite membrane maintained its superhydrophobicity with physical cross-links between the fibers and beads providing structural integrity, and displayed excellent flush resistance due to the stabilized composite structure.

## Supporting Information

Further experimental data and explanations are given upon (1) the GPC traces and corresponding molecular mass data of the SEBS, (2) SEM image of SEBS film by casting and its water CA measurement, (3) optical images and 3D surface topography images of a SEBS film and an electrospun SEBS fibrous mesh, (4) SEM image and 3D surface topography image of composite membrane consisted of fibers and Type I Beads, (5) TGA data of untreated and thermally annealed SEBS composite membranes (with Type II Beads).

## Acknowledgements

The authors thank the Science and Technology Planning Project of Guangzhou (No. 201510010133), the Fundamental Research Funds for the Central Universities (No. 2015ZP041) and the Pearl River Talents Scheme. PDT and LW thank the Royal Academy of Engineering (RAEng) for a Research Exchange Scheme grant between the UK and China. PDT also thanks the State Administration for Foreign Experts Affairs and the Royal Society of Chemistry for a Visiting Researcher Programme grant to China. The authors are grateful to the Shanghai Synchrotron Radiation Facility for providing synchrotron beam-time and thank the personnel of BL16B1 for their assistance.

## References

- [1] L. Jiang, Y. Zhao, J. Zhai, A lotus-leaf-like superhydrophobic surface: A porous microsphere/nanofiber composite film prepared by electrohydrodynamics, *Angew Chem Int Edit*, 43 (2004) 4338-4341.
- [2] R. Furstner, W. Barthlott, C. Neinhuis, P. Walzel, Wetting and self-cleaning properties of artificial superhydrophobic surfaces, *Langmuir*, 21 (2005) 956-961.
- [3] J. Zhu, C.M. Hsu, Z.F. Yu, S.H. Fan, Y. Cui, Nanodome Solar Cells with Efficient Light Management and Self-Cleaning, *Nano Letters*, 10 (2010) 1979-1984.
- [4] B. Bhushan, Y.C. Jung, Natural and biomimetic artificial surfaces for superhydrophobicity, self-cleaning, low adhesion, and drag reduction, *Prog Mater Sci*, 56 (2011) 1-108.
- [5] S. Nishimoto, B. Bhushan, Bioinspired self-cleaning surfaces with superhydrophobicity, superoleophobicity, and superhydrophilicity, *RSC Adv.*, 3 (2013) 671-690.

- [6] J.P. Zhang, S. Seeger, Polyester Materials with Superwetting Silicone Nanofilaments for Oil/Water Separation and Selective Oil Absorption, *Adv Funct Mater*, 21 (2011) 4699-4704.
- [7] X.Y. Zhang, Z. Li, K.S. Liu, L. Jiang, Bioinspired Multifunctional Foam with Self-Cleaning and Oil/Water Separation, *Adv Funct Mater*, 23 (2013) 2881-2886.
- [8] Z.X. Xue, Y.Z. Cao, N. Liu, L. Feng, L. Jiang, Special wettable materials for oil/water separation, *J. Mater. Chem. A*, 2 (2014) 2445-2460.
- [9] H.X. Wang, H. Zhou, H.T. Niu, J. Zhang, Y. Du, T. Lin, Dual-Layer Superamphiphobic/Superhydrophobic-Oleophilic Nanofibrous Membranes with Unidirectional Oil-Transport Ability and Strengthened Oil-Water Separation Performance, *Adv. Mater. Interfaces*, 2 (2015) 1400506.
- [10] X.D. Sun, V.G. Damle, A. Uppal, R. Linder, S. Chandrashekar, A.R. Mohan, K. Rykaczewski, Inhibition of Condensation Frosting by Arrays of Hygroscopic Antifreeze Drops, *Langmuir*, 31 (2015) 13743-13752.
- [11] X.D. Sun, V.G. Damle, S.L.Z. Liu, K. Rykaczewski, Bioinspired Stimuli-Responsive and Antifreeze-Secreting Anti-Icing Coatings, *Adv. Mater. Interfaces*, 2 (2015).
- [12] M.S. Khalil-Abad, M.E. Yazdanasheenas, Superhydrophobic antibacterial cotton textiles, *J Colloid Interf Sci*, 351 (2010) 293-298.
- [13] B.J. Privett, J. Youn, S.A. Hong, J. Lee, J. Han, J.H. Shin, M.H. Schoenfish, Antibacterial Fluorinated Silica Colloid Superhydrophobic Surfaces, *Langmuir*, 27 (2011) 9597-9601.
- [14] C.H. Xue, J. Chen, W. Yin, S.T. Jia, J.Z. Ma, Superhydrophobic conductive textiles with antibacterial property by coating fibers with silver nanoparticles, *Applied Surface Science*, 258 (2012) 2468-2472.
- [15] A.K. Kota, Y.X. Li, J.M. Mabry, A. Tuteja, Hierarchically Structured Superoleophobic Surfaces with Ultralow Contact Angle Hysteresis, *Adv Mater*, 24 (2012) 5838-5843.
- [16] A. Steele, I. Bayer, E. Loth, Inherently Superoleophobic Nanocomposite Coatings by Spray Atomization, *Nano Lett*, 9 (2009) 501-505.
- [17] M. Liu, F.-Q. Nie, Z. Wei, Y. Song, L. Jiang, In Situ Electrochemical Switching of Wetting State of Oil Droplet on Conducting Polymer Films, *Langmuir*, 26 (2009) 3993-3997.
- [18] C. Aulin, S.H. Yun, L. Wagberg, T. Lindstrom, Design of Highly Oleophobic Cellulose Surfaces from Structured Silicon Templates, *ACS Appl. Mater. Interfaces*, 1 (2009) 2443-2452.
- [19] L. Lin, M. Liu, L. Chen, P. Chen, J. Ma, D. Han, L. Jiang, Bio-Inspired Hierarchical Macromolecule-Nanoclay Hydrogels for Robust Underwater Superoleophobicity, *Adv Mater*, 22 (2010) 4826-4830.
- [20] K. Acatay, E. Simsek, C. Ow-Yang, Y.Z. Menceloglu, Tunable, superhydrophobically stable polymeric surfaces by electrospinning, *Angew Chem Int Edit*, 43 (2004) 5210-5213.
- [21] M.L. Ma, R.M. Hill, J.L. Lowery, S.V. Fridrikh, G.C. Rutledge, Electrospun poly(styrene-block-dimethylsiloxane) block copolymer fibers exhibiting superhydrophobicity, *Langmuir*, 21 (2005) 5549-5554.
- [22] J.F. Zheng, A.H. He, J.X. Li, J.A. Xu, C.C. Han, Studies on the controlled morphology and wettability of polystyrene surfaces by electrospinning or electrospraying, *Polymer*, 47 (2006) 7095-7102.
- [23] H. Wu, R. Zhang, Y. Sun, D.D. Lin, Z.Q. Sun, W. Pan, P. Downs, Biomimetic nanofiber patterns with controlled wettability, *Soft Matter*, 4 (2008) 2429-2433.
- [24] F. Li, Q.M. Li, H. Kim, Spray deposition of electrospun TiO<sub>2</sub> nanoparticles with self-cleaning and transparent properties onto glass, *Appl Surf Sci*, 276 (2013) 390-396.
- [25] M. Spasova, N. Manolova, N. Markova, I. Rashkov, Superhydrophobic PVDF and PVDF-

- HFP nanofibrous mats with antibacterial and anti-biofouling properties, *Appl Surf Sci*, 363 (2016) 363-371.
- [26] J. Yang, Z. Zhang, X. Men, X. Xu, X. Zhu, A simple approach to fabricate superoleophobic coatings, *New J Chem*, 35 (2011) 576-580.
- [27] J. Doshi, D.H. Reneker, *Electrospinning Process and Applications of Electrospun Fibers*, *J Electrostat*, 35 (1995) 151-160.
- [28] M. Bognitzki, W. Czado, T. Frese, A. Schaper, M. Hellwig, M. Steinhart, A. Greiner, J.H. Wendorff, Nanostructured fibers via electrospinning, *Adv Mater*, 13 (2001) 70-72.
- [29] L. Wang, C.M. Li, A.J. Ryan, S.P. Armes, Synthesis and peptide-induced degradation of biocompatible fibers based on highly branched poly(2-hydroxyethyl methacrylate), *Adv Mater*, 18 (2006) 1566-1570.
- [30] B. Ding, J. Lin, X. Wang, J. Yu, J. Yang, Y. Cai, Investigation of silica nanoparticle distribution in nanoporous polystyrene fibers, *Soft Matter*, 7 (2011) 8376-8383.
- [31] L.G. Wang, M. Wang, P.D. Topham, Y. Huang, Fabrication of magnetic drug-loaded polymeric composite nanofibres and their drug release characteristics, *RSC Adv.*, 2 (2012) 2433-2438.
- [32] U. Cengiz, M.Z. Avci, H.Y. Erbil, A.S. Sarac, Superhydrophobic terpolymer nanofibers containing perfluoroethyl alkyl methacrylate by electrospinning, *Appl Surf Sci*, 258 (2012) 5815-5821.
- [33] R.S. Kurusu, N.R. Demarquette, Blending and Morphology Control To Turn Hydrophobic SEBS Electrospun Mats Superhydrophilic, *Langmuir*, 31 (2015) 5495-5503.
- [34] X. Li, F.G. Bian, J.Y. Lin, Y.C. Zeng, Effect of electric field on the morphology and mechanical properties of electrospun fibers, *RSC Adv.*, 6 (2016) 50666-50672.
- [35] H. Fong, I. Chun, D.H. Reneker, Beaded nanofibers formed during electrospinning, *Polymer*, 40 (1999) 4585-4592.
- [36] L.G. Wang, P.D. Topham, O.O. Mykhaylyk, H. Yu, A.J. Ryan, J.P.A. Fairclough, W. Bras, Self-Assembly-Driven Electrospinning: The Transition from Fibers to Intact Beaded Morphologies, *Macromol Rapid Comm*, 36 (2015) 1437-1443.
- [37] A. Tuteja, W. Choi, J.M. Mabry, G.H. McKinley, R.E. Cohen, Robust omniphobic surfaces, *PNAS*, 105 (2008) 18200-18205.
- [38] M.W. Lee, S. An, B. Joshi, S.S. Latthe, S.S. Yoon, Highly Efficient Wettability Control via Three-Dimensional (3D) Suspension of Titania Nanoparticles in Polystyrene Nanofibers, *ACS Appl. Mater. Interfaces*, 5 (2013) 1232-1239.
- [39] D. Virovska, D. Paneva, N. Manolova, I. Rashkov, D. Karashanova, Electrospinning/electrospraying vs. electrospinning: A comparative study on the design of poly(L-lactide)/zinc oxide non-woven textile, *Appl Surf Sci*, 311 (2014) 842-850.
- [40] D. Virovska, D. Paneva, N. Manolova, I. Rashkov, D. Karashanova, Photocatalytic self-cleaning poly(L-lactide) materials based on a hybrid between nanosized zinc oxide and expanded graphite or fullerene, *Mat Sci Eng C-Mater*, 60 (2016) 184-194.
- [41] C.L. Su, Y.P. Li, Y.Z. Dai, F. Gao, K.X. Tang, H.B. Cao, Fabrication of three-dimensional superhydrophobic membranes with high porosity via simultaneous electrospraying and electrospinning, *Mater Lett*, 170 (2016) 67-71.
- [42] S.T. Yohe, M.W. Grinstaff, A facile approach to robust superhydrophobic 3D coatings via connective-particle formation using the electrospraying process, *Chem Commun*, 49 (2013) 804-806.
- [43] M. Wang, L. Wang, Y. Huang, Electrospun hydroxypropyl methyl cellulose phthalate

- (HPMCM/Erythromycin fibers for targeted release in intestine, *J Appl Polym Sci*, 106 (2007) 2177-2184.
- [44] L.G. Wang, J. Wu, Method of Preparation of Rinse-Resistant Superhydrophobic Composite Membranes, in: China Patent No. 201610634412x, China, 2016.
- [45] W. Rungswang, M. Kotaki, T. Shimojima, G. Kimura, S. Sakurai, S. Chirachanchai, Existence of microdomain orientation in thermoplastic elastomer through a case study of SEBS electrospun fibers, *Polymer*, 52 (2011) 844-853.
- [46] M. Kancheva, A. Toncheva, N. Manolova, I. Rashkov, Enhancing the mechanical properties of electrospun polyester mats by heat treatment, *Express Polym Lett*, 9 (2015) 49-65.
- [47] P. Li, J. Xie, Z. Deng, Characterization of irregularly micro-structured surfaces related to their wetting properties, *Appl Surf Sci*, 335 (2015) 29-38.
- [48] F. Tian, X.-H. Li, Y.-Z. Wang, C.-M. Yang, P. Zhou, J.-Y. Lin, J.-R. Zeng, C.-X. Hong, W.-Q. Hua, X.-Y. Li, X.-R. Miao, F.-G. Bian, J. Wang, Small angle X-ray scattering beamline at SSRF, *Nucl. Sci. Tech.*, 26 (2015) 030101.
- [49] J. Ilavsky, Nika: software for two-dimensional data reduction, *J. Appl. Crystallogr.*, 45 (2012) 324-328.
- [50] X.F. Wang, B. Ding, J.Y. Yu, M.R. Wang, Engineering biomimetic superhydrophobic surfaces of electrospun nanomaterials, *Nano Today*, 6 (2011) 510-530.
- [51] M. Ma, R.M. Hill, G.C. Rutledge, A Review of Recent Results on Superhydrophobic Materials Based on Micro- and Nanofibers, *J Adhes Sci Technol*, 22 (2008) 1799-1817.
- [52] Z.M. Huang, Y.Z. Zhang, M. Kotaki, S. Ramakrishna, A review on polymer nanofibers by electrospinning and their applications in nanocomposites, *Compos Sci Technol*, 63 (2003) 2223-2253.
- [53] W.E. Teo, S. Ramakrishna, A review on electrospinning design and nanofibre assemblies, *Nanotechnology*, 17 (2006) R89-R106.
- [54] P.W. Gibson, H.L. Schreuder-Gibson, D. Rivin, Electrospun fiber mats: Transport properties, *AIChE J.*, 45 (1999) 190-195.
- [55] H. Yoon, H. Kim, S.S. Latthe, M.-w. Kim, S. Al-Deyab, S.S. Yoon, A highly transparent self-cleaning superhydrophobic surface by organosilane-coated alumina particles deposited via electrospinning, *J. Mater. Chem. A*, 3 (2015) 11403-11410.
- [56] A. Tuteja, W. Choi, M. Ma, J.M. Mabry, S.A. Mazzella, G.C. Rutledge, G.H. McKinley, R.E. Cohen, Designing superoleophobic surfaces, *Science*, 318 (2007) 1618-1622.
- [57] L. Wang, P.D. Topham, O.O. Mykhaylyk, J.R. Howse, W. Bras, R.A.L. Jones, A.J. Ryan, Electrospinning pH-responsive block copolymer nanofibers, *Adv Mater*, 19 (2007) 3544-3548.
- [58] P.D. Topham, J.R. Howse, C.M. Fernyhough, A.J. Ryan, The performance of poly(styrene)-block-poly(2-vinyl pyridine)-block-poly(styrene) triblock copolymers as pH-driven actuators, *Soft Matter*, 3 (2007) 1506-1512.
- [59] P.D. Topham, J.R. Howse, C.J. Crook, A.J. Gleeson, W. Bras, S.P. Armes, R.A.L. Jones, A.J. Ryan, Autonomous volume transitions of a polybase triblock copolymer gel in a chemically driven pH-oscillator, *Macromol Symp*, 256 (2007) 95-104.